



Published in final edited form as:

Cancer Res. 2013 September 1; 73(17): 5381–5390. doi:10.1158/0008-5472.CAN-13-0033.

Notch1 induced brain tumor models the sonic hedgehog subgroup of human medulloblastoma

S. Natarajan^{a,1}, Y. Li^{a,1}, E.E. Miller^{a,1}, D. J Shih^b, M. D. Taylor^b, T. M. Stearns^a, R. T. Bronson^c, S. L. Ackerman^{a,d}, J. Yoon^e, and K. Yun^{1,2}

^aThe Jackson Laboratory, Bar Harbor, ME, USA

^bDivision of Neurosurgery, Program in Developmental and Stem Cell Biology, Hospital for Sick Children, Toronto, Canada

^cDana Farber Cancer Institute, Boston, MA, USA

^dHoward Hughes Medical Institute

^eMaine Medical Center Research Institute, Scarborough, ME, USA

Abstract

While activation of the Notch pathway is observed in many human cancers, it is unknown whether elevated *Notch1* expression is sufficient to initiate tumorigenesis in most tissues. To test the oncogenic potential of *Notch1* in solid tumors, we expressed an activated form of NOTCH1 (NIICD) in the developing mouse brain. *NIICD;hGFAP-cre* mice were viable but developed severe ataxia and seizures, and died by weaning age. Analysis of transgenic embryonic brains revealed that NIICD expression induced p53-dependent apoptosis. When apoptosis was blocked by genetic deletion of p53, 30~40% of *NIICD;GFAP-cre;p53+/-* and *NIICD;GFAP-cre;p53-/-* mice developed spontaneous medulloblastomas. Interestingly, *Notch1*-induced medulloblastomas most closely resembled the sonic hedgehog (SHH) subgroup of human medulloblastoma at the molecular level. Surprisingly, NIICD-induced tumors do not maintain high levels of the Notch pathway gene expression, except for *Notch2*, demonstrating that initiating oncogenic events may not be decipherable by analyzing growing tumors in some cases. In summary, this study demonstrates that *Notch1* has an oncogenic potential in the brain when combined with other oncogenic hits, such as p53 loss, and provides a novel mouse model of medulloblastoma.

Introduction

The Notch pathway is a highly conserved signaling pathway that is essential for normal development, and is implicated in both somatic stem cell homeostasis and human cancer (1–4). The canonical Notch pathway mediates cell-cell communication among adjacent cells that are in direct contact with one another, through membrane-bound ligand-receptor interactions (juxtacrine signaling). When a ligand (DELTA and JAGGED family members) binds to NOTCH receptors (NOTCH1 - 4 in mammals), NOTCH is cleaved through highly controlled step-wise processes, and the intracellular domain of NOTCH (NICD) is released from the membrane and enters the nucleus to form a transcriptional complex. In the nucleus, NICD displaces repressive co-factors bound to RBPJ and recruits MAML to turn on expression of downstream target genes, including *Hes1*, *Hes5*, *Hey1*, and *Hey2* (5).

²Corresponding author: Kyuson Yun, The Jackson Laboratory, 600 Main St., Bar Harbor, ME, 04609, USA, Kyuson.yun@jax.org, Tel: 207-288-6825.

¹These authors contributed equally to this work.

There is not conflict of interest to report by any of the authors.

A growing body of evidence implicates the Notch pathway in human cancers. For example, >50% of T-ALL (T-cell Acute Lymphoblastic Leukemia) patients have activating mutations in the *Notch1* gene (6, 7), indicating that *Notch1* has oncogenic potential in the hematopoietic system. While activating mutations in *Notch* genes have not been widely reported in solid cancers, Notch pathway activity level is high in many solid cancers, including brain cancers (2, 3, 8).

Medulloblastoma is the most common form of pediatric brain tumor and is considered a classical example of a developmental cancer. They are thought to arise from abnormal proliferation of EGL progenitors in the cerebellum (9), although there is evidence that neural stem cells (NSCs) can also be transformed to give rise to medulloblastomas (10, 11). Genetically, two key developmental signaling pathways, WNT and SHH pathways, have been implicated in heritable forms of medulloblastoma, Turcot's syndrome, and Gorlin syndrome, respectively (12, 13). Although the Notch pathway is not genetically linked to medulloblastomas, several lines of evidence implicate the Notch pathway in medulloblastoma pathogenesis. First, *NOTCH2* RNA level is reported to be higher in medulloblastomas than normal fetal brain, and *NOTCH2* and *HES1* expression levels significantly correlate with shorter survival time among medulloblastoma patients (14). Second, ~15% of PNET and medulloblastomas contained amplification of the genomic region containing the *NOTCH2* gene (14), and recent sequencing studies of medulloblastoma genome identified mutations within the *NOTCH3* and *NOTCH4* genes (15, 16). Third, Notch signaling is necessary to maintain cancer stem cells in brain tumors: inhibition of the Notch pathway leads to reduced self-renewal, tumorigenic capacity, and radio-resistance of medulloblastoma and glioma stem cells (17–20). Together, these studies suggest that aberrant activation of the Notch pathway may lead to tumor formation in the brain; however, the oncogenic potential of Notch pathway activation has not yet been demonstrated experimentally (21–25).

In this study, we provide *in vivo* evidence that aberrant Notch pathway activation can be an initiating oncogenic event in the brain. We used a transgenic approach to express a constitutively activated form of *Notch1* (N1ICD) in the developing mouse brain, and show that while N1ICD expression alone is not sufficient to cause brain tumor formation, N1ICD expression accompanied by loss of single or both copies of p53 results in medulloblastoma formation.

Results

Ectopic N1ICD expression results in abnormal brain development

To determine whether *Notch1* can act as an oncogene in the brain, we conditionally expressed a constitutively activate form of *Notch1*, N1ICD, in the developing mouse brain using a Cre-lox system (Fig. 1A). When *N1ICD* mice were crossed to *hGFAP-cre* mice, the double transgenic (*N1ICD;hGFAP-cre*) embryos showed high expression of the transgene in the developing brain (Fig. 1B). Realtime RT-PCR analysis of *N1ICD;hGFAP-cre* and control littermate cortices and cerebella at E15.5 confirmed elevated level of *N1ICD* and Notch pathway target genes, *Hes1*, *Hes5*, *Hey1*, and *Hey2* at the RNA level in transgenic brains (Fig. 1C, D). *N1ICD;hGFAP-cre* mice were viable but developed severe ataxia and seizures by weaning age, and all mice died by 4 weeks of age (Fig. 1E). Gross morphological examination of brains from postnatal day 20 control and *N1ICD;hGFAP-cre* littermates showed severely hypoplastic brains in transgenic mice compared to controls (Fig. 1F). Histological analysis showed that transgenic brains were characterized by severely hypoplastic hippocampus lacking dentate gyrus, thinner and disorganized cortical layers with reduced number of neurons, and grossly hypoplastic cerebellum with obvious heterotopia of granule cells (Fig. 1G).

To identify the developmental origin of these brain defects, we examined *NIICD;hGFAP-cre* and control littermate brains at E15.5, three days after the Cre recombinase expression and the peak of neurogenesis in the cerebral cortex. NIICD was robustly expressed in proliferating and differentiating cells of the cortex, as indicated by the Myc-tag expression in KIi67+ proliferating cells (Fig. 2A) and MAP2+ differentiating neurons (Fig. 2B). Cell-type specific analyses with antibodies marking NSCs (SOX2, PAX6), intermediate progenitors (TBR2, Neurogenin2), and neurons (MAP2, NeuN, β -3-tubulin) showed greatly reduced numbers of all three cell types in transgenic cortices (Fig. 2C, D, E and not shown). In addition, analyses with markers for cellular proliferation (phospho-Histone 3, BrdU) showed reduced proliferation (Fig. 2F) and a marker for apoptosis (cleaved caspase3) showed concurrent increase in the number of apoptotic cells (Fig. 2G).

Similar to cortex, Myc+ cells were observed in the neuroepithelium and in PAX6+ EGL progenitor cells in the developing cerebellum (Fig. 3A, B). At E15.5, increased apoptosis and reduced proliferation resulted in decreased numbers of PAX6+ neural precursor cells in the transgenic cerebellum, compared to littermate control (Fig. 3C, D, E). Together, these results indicate that hypoplasia observed in *NIICD;hGFAP-cre* brain regions arise from both increased cell death and early loss of proliferating stem and progenitor cells.

NIICD expression activates the p53 pathway *in vivo*

To understand the molecular basis for these brain phenotypes, we performed a transcriptome analysis of control and *NIICD;hGFAP-cre* littermate cortices from E13.5 embryos, one day after the Cre recombinase is activated in the developing cortex. Only five genes (*Akr1b3*, *Eda2r*, *Ccng1*, *Gpr75*, and *LOC100041678*) were identified to show statistically significant expression changes ($q < 0.05$, relative fold change (RFC) $> \pm 2$). The small number of differentially expressed genes observed is likely due to the variable severity of phenotypes in individual transgenic samples and the brevity of transgene expression at the time of analysis, which was designed to capture the earliest gene expression changes. Realtime RT-PCR analyses on independent sets of samples confirmed increased expression of *Akr1b3*, *Eda2r*, *Ccng1* and *Gpr75* in *NIICD;hGFAP-cre* cortices (Fig. 4A). Interestingly, *Ccng1* is involved in G2/M arrest in response to DNA damage, and subsequent cellular proliferation (26); further, *Ccng1* and *Eda2r* are transcriptional targets of the p53 tumor suppressor gene (27, 28). These results suggest that ectopic expression of NIICD might induce genotoxic stress that activates the p53 pathway.

To test this hypothesis, we examined p53 activation and its target gene expression in control and *NIICD;hGFAP-cre* transgenic brains at E15.5. p53 protein level, assessed by immunofluorescence analysis, was elevated in transgenic cortices compared to control littermates (Fig. 4B), indicating activation of the p53 pathway. We also detected increased expression of *p21*, a downstream effector of p53 that mediates DNA damage response and apoptosis (Fig. 4C). Together, these results suggest that the observed increase in apoptosis in *NIICD;hGFAP-cre* brains is mediated through the p53 pathway.

Loss of p53 rescues NIICD-induced apoptosis and premature gliogenesis

To genetically test whether the increased apoptosis in *NIICD;hGFAP* brains was indeed induced by the p53 pathway, we analyzed *NIICD;hGFAP-cre;p53^{+/-}* and *NIICD;hGFAP-cre;p53^{-/-}* brains at E15.5. Apoptosis was blocked in brains of *NIICD;hGFAP-cre;p53^{-/-}* mice as anticipated. Interestingly, the number of apoptotic cells was also greatly reduced in *NIICD;hGFAP-cre;p53^{+/-}* brains, as indicated by significant reductions in the number of TUNEL+ or cleaved Caspase3+ cells (Fig. 4D, E, Supplementary Fig. 1).

To determine whether blocking p53-mediated apoptosis is sufficient to rescue the neurological phenotype and premature death of *NIICD;hGFAP-cre* mice (Fig. 1E), we generated postnatal *NIICD;hGFAP-cre;p53+/-* and *NIICD;hGFAP-cre;p53-/-* mice and aged them. Consistent with apoptosis marker analyses, loss of one copy of p53 was sufficient to rescue early lethality to an extent similar to that by loss of both copies of p53 (Fig. 4F). Gross analysis of wean age (P20) brains showed observable rescue in brain sizes in *p53+/-* and *p53-/-* transgenic brains, particularly in the cortex (Supplementary Fig. 2).

Although loss of p53 rescued the size of NIICD transgenic brains to a large extent, >50% of *NIICD;hGFAP-cre;p53-/-* and *NIICD;hGFAP-cre;p53+/-* mice still died by 4 months of age with neurological phenotypes (Fig. 4F). Since previous studies have reported that ectopic NIICD expression in the developing nervous system induces precocious expression of GFAP, a marker for astrocytes (25, 29), we tested whether premature gliogenesis is responsible for the neurological phenotype in p53 mutant transgenic mice. Analysis of GFAP expression in transgenic mice with 0, 1, or 2 copies of p53 showed that loss of p53 expression also blocked precocious GFAP expression in both *NIICD;hGFAP-cre;p53-/-* and *NIICD;hGFAP-cre;p53+/-* mice (Supplementary Fig. 3). This observation suggests that premature gliogenesis is not likely to be the major cause of death or neural phenotypes in *NIICD;hGFAP-cre;p53+/-* and *NIICD;hGFAP-cre;p53-/-* mice. Furthermore, it suggests that aberrant activation of GFAP expression by NIICD expression *in vivo* requires a p53.

***NIICD;GFAP-cre;p53-/-* and *NIICD;GFAP-cre;p53+/-* mice develop medulloblastomas**

To further investigate the cause of death of *NIICD;hGFAP-cre;p53+/-* and *NIICD;hGFAP-cre;p53-/-* mice, we analyzed weaning-age brains of *NI-ICD;hGFAP-cre* transgenic mice with 0, 1, or 2 copies of the *p53* gene. We observed heterotopia in a subset of *NIICD;hGFAP-cre* transgenic brains, regardless of the p53 status (Fig. 5A). Notably, we also observed medulloblastomas in transgenic mice lacking one or both copies of p53 (Fig. 5A). Histologically, 11 of 12 tumors analyzed showed classical medulloblastoma histology, composed primarily of small EGL progenitor-like cells (Fig. 5B, Supplementary Fig 4). One mouse showed different tumor histology, resembling a large-cell anaplastic medulloblastoma (Fig. 4C). Immunohistochemical analyses showed that NIICD-induced tumors are highly proliferative (Ki67+), with most cells expressing the early neural stem/progenitor marker OLIG2 (Fig. 4D). Many tumor cells expressed an EGL progenitor marker, ATOH1/MATH1, and a neuronal marker, NeuN (Fig. 4D), but not the glia marker GFAP, confirming that these tumors are medulloblastomas. Interestingly, only a small number of tumor cells continued to express the transgene, as indicated by Myc antibody staining (Fig. 4D). Interestingly, no other types of brain tumors were observed in the *NIICD;hGFAP-cre;p53-/-* and *NIICD;hGFAP-cre;p53+/-* mice, even though other regions of the brain contained a large number of apoptotic cells in *NIICD;hGFAP-cre* embryos (Fig 2G and not shown).

NIICD-induced medulloblastomas most closely resemble the SHH subgroup of human medulloblastomas

Currently, human medulloblastomas are categorized into four molecular subgroups: WNT, Sonic Hedgehog (SHH), Group 3 and Group 4 (30). Elevated Notch pathway activity has been observed in a subset of human medulloblastomas but is not associated with any given molecular subgroup (31). To determine whether NIICD-induced tumors model a particular molecular subgroups of human medulloblastomas, we performed a transcriptome analysis of NIICD-induced tumors and assessed the expression of signature genes of the four human medulloblastoma molecular subgroups. Surprisingly, NIICD-induced medulloblastomas most closely matched the gene signature associated with the SHH-subgroup of human medulloblastomas (Fig. 6A,B).

To confirm the SHH subgroup categorization of N1ICD-induced medulloblastomas, we performed realtime RT-PCR analyses, comparing the tumors to wildtype postnatal day 8 cerebella of C57BL/6J (B6) mice. As shown in Figure 6C, the SHH pathway genes *Gli1*, *Gli2*, and *Ptch2* were highly expressed in N1ICD medulloblastomas. Consistent with microarray data (Fig. 6A) and the antibody staining (Fig. 5D), *Atoh1/Math1*, a marker for EGL progenitors, was also significantly increased in N1ICD tumors at the RNA level (Fig. 6C). In addition, we observed significantly increased expression of cell cycle regulators, *Cyclins D1*, *D2*, and *E2* in N1ICD tumors (Fig. 6D). These results are consistent with the histological analysis showing that N1ICD tumors are composed of highly proliferative cells resembling EGL progenitors and the SHH subgroup designation. Surprisingly, most of the Notch pathway genes were not highly expressed in the bulk tumor cells (Fig. 6E). In particular, *N1ICD* level was not significantly up-regulated at the bulk tumor level, consistent with the immunohistochemical analysis that only a small number of cells continue to express the transgene in the tumor (Fig. 5D). On the other hand, *Notch2*, normally expressed in EGL progenitor cells and shown to promote their proliferation (32), was higher expressed in tumors, supporting the idea that bulk tumor cells are mostly composed of EGL-progenitor like cells. Interestingly, genes that were identified to be downstream of N1ICD expression in *N1ICD;hGFAP-cre* cerebral cortices at E13.5 (*Ccng1*, *Eda2r*, *Akr1b3*, *LOC1000041678*) were also highly elevated in the tumors (Fig. 6F), suggesting that these genes were also activated in the developing cerebellum upon N1ICD expression and maintained in the tumor. Together, these marker analyses suggest that most N1ICD medulloblastomas are composed of EGL progenitor-like cells that have high levels of *Atoh1*, *Ptch2*, *Gli1* and *Gli2* expression, and that N1ICD induced tumor may model a subset of SHH subgroup of human medulloblastomas.

DISCUSSION

Notch pathway activation is observed in many human cancers, including brain cancer (2, 3). In addition, it has been shown to be necessary for maintaining brain cancer stem cells from gliomas and medulloblastomas *in vitro* and *in vivo* (17–19). To directly test whether *Notch1* has the potential in brain tumor initiation, we generated a mouse model in which activated *Notch1* is expressed in the developing brain. Similar to over-expression of Notch2-ICD in the brain (23), N1ICD over-expression alone was not sufficient to induce brain tumors. However, 10–60% of *N1ICD;hGFAP-cre;p53+/-* and *N1ICD;hGFAP-cre;p53-/-* mice developed medulloblastomas (Fig. 5A). Hence, this study demonstrates that elevated *Notch1* activity, when combined with cooperating oncogenic events, can be an initiating oncogenic hit in the mammalian brain.

Interestingly, while we observed p53-mediated apoptosis in all regions of the brain in *N1ICD;hGFAP-cre* mice, we did not observe any brain tumor types other than medulloblastomas in *N1ICD;hGFAP-cre;p53+/-* and *N1ICD;hGFAP-cre;p53-/-* mice. Previous analyses of mice with mutations in the DNA-damage-repair pathway genes also reported similar occurrences of medulloblastomas (and not of other brain tumors) on p53 mutant backgrounds (33–36). This is consistent with our observation that the major cellular response to N1ICD expression is a DNA damage response (Fig. 4). Together, these results suggest that cerebellar cells may be more sensitive to DNA damage-induced cellular transformation in comparison to cells in other brain regions. Alternatively, there may be a selection against other types of tumors, such as gliomas, that would cause embryonic lethality if they developed *in utero*, or that would have formed in older mice. However, the latter possibility is unlikely, as we did not observe other types of brain tumor in any of the older *N1ICD;hGFAP-Cre;p53+/-* and *N1ICD;hGFAP-Cre;p53-/-* mice we examined, although we did observe nasal epithelial tumors in some mice.

High-level Notch pathway activity, in contrast to Wnt or SHH pathway activity, does not identify a specific subgroup of human medulloblastomas (31). However, N1ICD-induced medulloblastomas express high levels of the SHH-pathway genes, categorizing the tumors as models for the SHH subgroup of human medulloblastomas (Fig. 6). Interestingly, previous studies have shown that Notch pathway activity is dispensable for SHH-induced medulloblastoma initiation or maintenance (37, 38). While it remains to be determined whether Notch pathway cooperates with other oncogenic pathways, our study clearly indicates that Notch activation is a strong inducer of medulloblastomas in p53 mutant backgrounds. Notably, p53 mutations are observed in 12–14% of WNT and SHH subgroups of human medulloblastomas (39), suggesting that this model is physiologically relevant. Our observation that p53 functions downstream of N1ICD to modulates *Notch1* target gene expression, such as GFAP (Supplementary Fig. 3), suggests that p53 interaction with the Notch pathway *in vivo* may be more complicated than is currently known.

In the future, it will be important to further elucidate the molecular mechanism of cellular transformation induced by Notch1 activation. Consistent with earlier studies performed on bone marrow cells (40, 41), N-terminal truncation (deletion of the RAM domain) of the N1ICD protein analyzed in this study did not affect cellular transformation or target gene expression. In support of this conclusion, we observed similar increase in apoptosis and reduced numbers of proliferating stem/progenitor cells in the brain of another allele of N1ICD transgenic mouse that expressed human N1ICD that contains the RAM domain (Supplementary Fig 5, 6, (25)). Interestingly, our analysis of yet another allele of N1ICD transgenic mouse in which N1ICD lacking the PEST domain was knocked into the ROSA locus showed increased neural stem cell expansion but not increased apoptosis or tumorigenesis (24). Together, results of these studies show that Notch pathway activation *in vivo* results in drastically different biological outcome depending on the cellular context and the domains and/or dose of N1ICD expression. Comparisons of these different alleles of N1ICD transgenic mice will be useful in elucidating the molecular mechanism of *Notch1* function in stem cell maintenance and cellular transformation.

In summary, we demonstrate that *Notch1* can be an oncogene in the brain and that elevation of Notch pathway activation in p53-deficient mice generates a novel mouse model of medulloblastoma. Interestingly, these tumors most closely resemble the SHH-subgroup of human medulloblastomas and show high levels of the SHH pathway activity. Unexpectedly while we observe high levels of *Notch2* expression in these tumors, consistent with normal *Notch2* expression in EGL progenitor cells (32), we did not detect high-level expression of other Notch pathway components. This observations suggests a hit-and-run or some other mechanism of oncogenesis by *N1ICD* that does not require sustained expression of *N1ICD* in growing tumor cells, such as non-cell-autonomous effect of p53 recently reported (42). It also suggests the possibility that Notch pathway may play a significant role in tumor initiation (but not maintenance) in other tissues in which the Notch pathway plays a critical role in stem/progenitor cell proliferation and survival. Finally, our results suggest that a molecular signature of the initiating oncogenic event is not necessarily preserved in established tumors and that analysis of dominant maintenance pathway in growing, bulk tumor cells may not be informative in elucidating early oncogenic events in some tumors.

MATERIALS AND METHODS

Animals

All mice were treated according to the guidelines of The Jackson Laboratory and The Jackson Laboratory Animal Care and Usage Committee approved all procedures. We analyzed two different founder transgenic N1ICD lines (N1ICD-43 and N1ICD-29) that were generated in Jeong Yoon's laboratory at MMCRI (43), and observed the same

phenotype in both lines. In these mice, intracellular domain of mouse Notch1 minus the RAM domain (aa 1810-2531) is conditionally expressed upon Cre excision (Supplementary Fig 6). p53 (B6.129S2-*Trp53tm1Tyj/J*; JR#2101), *GFAP-cre* (JAX FVB-Tg(*GFAP-cre*)25Mes/J; JR#4600), and *ACTB-Notch1* (C57BL/6J-Tg(*ACTB-NOTCH1*)1Shn/J; human N1ICD: JR#6481) mice were obtained from The Jackson Laboratory Repository. All analyses were performed by comparing littermates to minimize variability and in a minimum of three independent sets of samples.

Immunohistochemistry/immunofluorescence

Standard immunohistochemistry and immunofluorescence protocols were used with antibodies listed in the Supplementary Methods section on either frozen and/or paraffin sections.

Microarray analysis

Affymetrix ST1.0 chips were used with 3 independent sets of samples from control and *N1ICD;hGFAP-cre* E13.5 cortices from littermates or from 4 independent *N1ICD;hGFAP-cre;p53* tumors. For analytical details, please see Supplementary Methods.

Realtime RT-PCR

To measure relative RNA levels of control and transgenic cortices or tissues, total RNA was isolated using Trizol. Genomic DNA was removed by treating RNA samples with DNase following the recommended protocol from Ambion (TURBO DNA-free™, Ambion). cDNAs were generated using the iScript kit from BioRad, and primers specific for each target gene (see Supplementary Methods) were used with SYBR green reaction mix from BioRad. All reactions were run in triplicates, and 18S levels were used to normalize samples to one another. Relative fold change compared to wildtype control is presented in all figures.

Supplementary Material

Refer to Web version on PubMed Central for supplementary material.

Acknowledgments

We thank Jane Johnson for providing the MATH1 antibody, Jesse Hammer for assistance with figures, Gene Expression Service at JAX for Affymetrix analysis, Stephen Sampson for manuscript editing, Patsy Nishina and Kevin Mills for critical reading of the manuscript, and members of the Yun lab for their support. This work was supported in part by the Maine Cancer Foundation and TJJ Cancer Center Support grant CA034196 to KY. SLA is an investigator of the Howard Hughes Medical Institute.

References

1. Allenspach EJ, Maillard I, Aster JC, Pear WS. Notch signaling in cancer. *Cancer biology & therapy*. 2002; 1:466–76. [PubMed: 12496471]
2. Koch U, Radtke F. Notch signaling in solid tumors. *Curr Top Dev Biol*. 2010; 92:411–55. [PubMed: 20816403]
3. Pierfelice TJ, Schreck KC, Eberhart CG, Gaiano N. Notch, neural stem cells, and brain tumors. *Cold Spring Harb Symp Quant Biol*. 2008; 73:367–75. [PubMed: 19022772]
4. Pierfelice T, Alberi L, Gaiano N. Notch in the vertebrate nervous system: an old dog with new tricks. *Neuron*. 2011; 69:840–55. [PubMed: 21382546]
5. Kopan R, Ilagan MX. The canonical Notch signaling pathway: unfolding the activation mechanism. *Cell*. 2009; 137:216–33. [PubMed: 19379690]
6. Aster JC, Pear WS, Blacklow SC. Notch signaling in leukemia. *Annu Rev Pathol*. 2008; 3:587–613. [PubMed: 18039126]

7. Weng AP, Ferrando AA, Lee W, Morris JPt, Silverman LB, Sanchez-Irizarry C, et al. Activating mutations of NOTCH1 in human T cell acute lymphoblastic leukemia. *Science*. 2004; 306:269–71. [PubMed: 15472075]
8. Purow BW, Haque RM, Noel MW, Su Q, Burdick MJ, Lee J, et al. Expression of Notch-1 and its ligands, Delta-like-1 and Jagged-1, is critical for glioma cell survival and proliferation. *Cancer Res*. 2005; 65:2353–63. [PubMed: 15781650]
9. Behesti H, Marino S. Cerebellar granule cells: insights into proliferation, differentiation, and role in medulloblastoma pathogenesis. *Int J Biochem Cell Biol*. 2009; 41:435–45. [PubMed: 18755286]
10. Yang ZJ, Ellis T, Markant SL, Read TA, Kessler JD, Bourbonoulas M, et al. Medulloblastoma can be initiated by deletion of Patched in lineage-restricted progenitors or stem cells. *Cancer Cell*. 2008; 14:135–45. [PubMed: 18691548]
11. Schuller U, Heine VM, Mao J, Kho AT, Dillon AK, Han YG, et al. Acquisition of granule neuron precursor identity is a critical determinant of progenitor cell competence to form Shh-induced medulloblastoma. *Cancer Cell*. 2008; 14:123–34. [PubMed: 18691547]
12. Hamilton SR, Liu B, Parsons RE, Papadopoulos N, Jen J, Powell SM, et al. The molecular basis of Turcot's syndrome. *N Engl J Med*. 1995; 332:839–47. [PubMed: 7661930]
13. Johnson RL, Rothman AL, Xie J, Goodrich LV, Bare JW, Bonifas JM, et al. Human homolog of patched, a candidate gene for the basal cell nevus syndrome. *Science*. 1996; 272:1668–71. [PubMed: 8658145]
14. Fan X, Mikolaenko I, Elhassan I, Ni X, Wang Y, Ball D, et al. Notch1 and notch2 have opposite effects on embryonal brain tumor growth. *Cancer research*. 2004; 64:7787–93. [PubMed: 15520184]
15. Pugh TJ, Weeraratne SD, Archer TC, Pomeranz Krummel DA, Auclair D, Bochicchio J, et al. Medulloblastoma exome sequencing uncovers subtype-specific somatic mutations. *Nature*. 2012
16. Jones DT, Jager N, Kool M, Zichner T, Hutter B, Sultan M, et al. Dissecting the genomic complexity underlying medulloblastoma. *Nature*. 2012; 488:100–5. [PubMed: 22832583]
17. Fan X, Matsui W, Khaki L, Stearns D, Chun J, Li YM, et al. Notch pathway inhibition depletes stem-like cells and blocks engraftment in embryonal brain tumors. *Cancer Res*. 2006; 66:7445–52. [PubMed: 16885340]
18. Fan X, Khaki L, Zhu TS, Soules ME, Talsma CE, Gul N, et al. NOTCH pathway blockade depletes CD133-positive glioblastoma cells and inhibits growth of tumor neurospheres and xenografts. *Stem Cells*. 2010; 28:5–16. [PubMed: 19904829]
19. Hovinga KE, Shimizu F, Wang R, Panagiotakos G, Van Der Heijden M, Moayedpardazi H, et al. Inhibition of notch signaling in glioblastoma targets cancer stem cells via an endothelial cell intermediate. *Stem Cells*. 2010; 28:1019–29. [PubMed: 20506127]
20. Wang J, Wakeman TP, Lathia JD, Hjelmeland AB, Wang XF, White RR, et al. Notch promotes radioresistance of glioma stem cells. *Stem Cells*. 2010; 28:17–28. [PubMed: 19921751]
21. Dang L, Fan X, Chaudhry A, Wang M, Gaiano N, Eberhart CG. Notch3 signaling initiates choroid plexus tumor formation. *Oncogene*. 2006; 25:487–91. [PubMed: 16186803]
22. Pierfelice TJ, Schreck KC, Dang L, Asnaghi L, Gaiano N, Eberhart CG. Notch3 activation promotes invasive glioma formation in a tissue site-specific manner. *Cancer research*. 2011; 71:1115–25. [PubMed: 21245095]
23. Tchorz JS, Tome M, Cloetta D, Sivasankaran B, Grzmil M, Huber RM, et al. Constitutive Notch2 signaling in neural stem cells promotes tumorigenic features and astroglial lineage entry. *Cell Death Dis*. 2012; 3:e325. [PubMed: 22717580]
24. Li Y, Hibbs MA, Gard AL, Shylo NA, Yun K. Genome-Wide Analysis of N1ICD/RBPJ Targets in vivo Reveals Direct Transcriptional Regulation of Wnt, SHH, and Hippo Pathway Effectors by Notch1. *Stem Cells*. 2012
25. Yang X, Klein R, Tian X, Cheng HT, Kopan R, Shen J. Notch activation induces apoptosis in neural progenitor cells through a p53-dependent pathway. *Dev Biol*. 2004; 269:81–94. [PubMed: 15081359]
26. Kimura SH, Ikawa M, Ito A, Okabe M, Nojima H. Cyclin G1 is involved in G2/M arrest in response to DNA damage and in growth control after damage recovery. *Oncogene*. 2001; 20:3290–300. [PubMed: 11423978]

27. Okamoto K, Beach D. Cyclin G is a transcriptional target of the p53 tumor suppressor protein. *The EMBO journal*. 1994; 13:4816–22. [PubMed: 7957050]
28. Brosh R, Sarig R, Natan EB, Molchadsky A, Madar S, Bornstein C, et al. p53-dependent transcriptional regulation of EDA2R and its involvement in chemotherapy-induced hair loss. *FEBS letters*. 2010; 584:2473–7. [PubMed: 20434500]
29. Morrison SJ, Perez SE, Qiao Z, Verdi JM, Hicks C, Weinmaster G, et al. Transient Notch activation initiates an irreversible switch from neurogenesis to gliogenesis by neural crest stem cells. *Cell*. 2000; 101:499–510. [PubMed: 10850492]
30. Taylor MD, Northcott PA, Korshunov A, Remke M, Cho YJ, Clifford SC, et al. Molecular subgroups of medulloblastoma: the current consensus. *Acta neuropathologica*. 2012; 123:465–72. [PubMed: 22134537]
31. Kool M, Koster J, Bunt J, Hasselt NE, Lakeman A, van Sluis P, et al. Integrated genomics identifies five medulloblastoma subtypes with distinct genetic profiles, pathway signatures and clinicopathological features. *PLoS ONE*. 2008; 3:e3088. [PubMed: 18769486]
32. Solecki DJ, Liu XL, Tomoda T, Fang Y, Hatten ME. Activated Notch2 signaling inhibits differentiation of cerebellar granule neuron precursors by maintaining proliferation. *Neuron*. 2001; 31:557–68. [PubMed: 11545715]
33. Lee Y, McKinnon PJ. DNA ligase IV suppresses medulloblastoma formation. *Cancer research*. 2002; 62:6395–9. [PubMed: 12438222]
34. Tong WM, Ohgaki H, Huang H, Granier C, Kleihues P, Wang ZQ. Null mutation of DNA strand break-binding molecule poly(ADP-ribose) polymerase causes medulloblastomas in p53(–/–) mice. *The American journal of pathology*. 2003; 162:343–52. [PubMed: 12507917]
35. Frappart PO, Lee Y, Russell HR, Chalhoub N, Wang YD, Orii KE, et al. Recurrent genomic alterations characterize medulloblastoma arising from DNA double-strand break repair deficiency. *Proceedings of the National Academy of Sciences of the United States of America*. 2009; 106:1880–5. [PubMed: 19164512]
36. Yan CT, Kaushal D, Murphy M, Zhang Y, Datta A, Chen C, et al. XRCC4 suppresses medulloblastomas with recurrent translocations in p53-deficient mice. *Proc Natl Acad Sci U S A*. 2006; 103:7378–83. [PubMed: 16670198]
37. Julian E, Dave RK, Robson JP, Hallahan AR, Wainwright BJ. Canonical Notch signaling is not required for the growth of Hedgehog pathway-induced medulloblastoma. *Oncogene*. 2010; 29:3465–76. [PubMed: 20418906]
38. Hatton BA, Villavicencio EH, Pritchard J, LeBlanc M, Hansen S, Ulrich M, et al. Notch signaling is not essential in sonic hedgehog-activated medulloblastoma. *Oncogene*. 2010; 29:3865–72. [PubMed: 20440271]
39. Northcott PA, Jones DT, Kool M, Robinson GW, Gilbertson RJ, Cho YJ, et al. Medulloblastomics: the end of the beginning. *Nature reviews Cancer*. 2012; 12:818–34.
40. Aster JC, Xu L, Karnell FG, Patriub V, Pui JC, Pear WS. Essential roles for ankyrin repeat and transactivation domains in induction of T-cell leukemia by notch1. *Molecular and cellular biology*. 2000; 20:7505–15. [PubMed: 11003647]
41. Aster JC, Robertson ES, Hasserjian RP, Turner JR, Kieff E, Sklar J. Oncogenic forms of NOTCH1 lacking either the primary binding site for RBP-Jkappa or nuclear localization sequences retain the ability to associate with RBP-Jkappa and activate transcription. *The Journal of biological chemistry*. 1997; 272:11336–43. [PubMed: 9111040]
42. Lujambio A, Akkari L, Simon J, Grace D, Tschaharganeh DF, Bolden JE, et al. Non-Cell-Autonomous Tumor Suppression by p53. *Cell*. 2013; 153:449–60. [PubMed: 23562644]
43. Venkatesh DA, Park KS, Harrington A, Miceli-Libby L, Yoon JK, Liaw L. Cardiovascular and hematopoietic defects associated with Notch1 activation in embryonic Tie2-expressing populations. *Circulation research*. 2008; 103:423–31. [PubMed: 18617694]

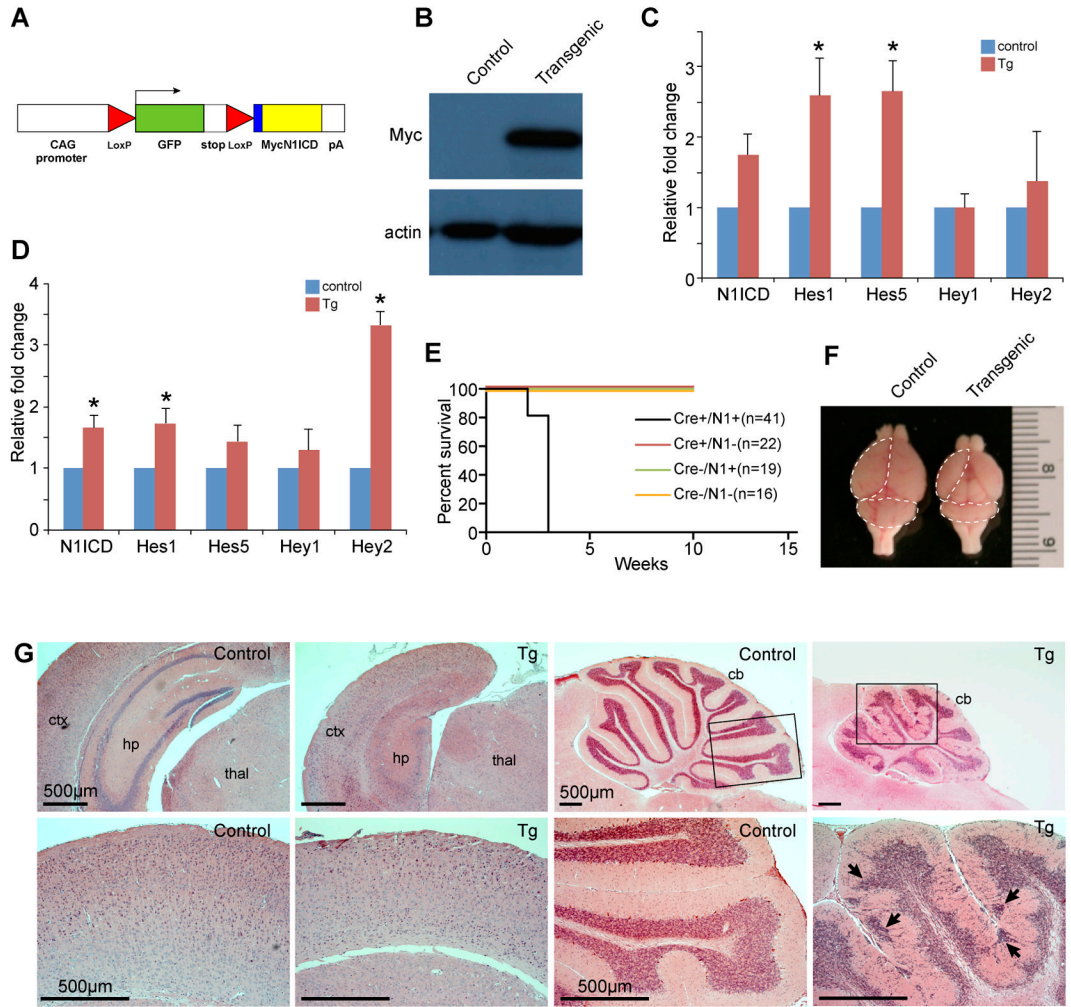


Figure 1. Ectopic N1ICD expression in the developing brain results in ataxia, seizures, and early lethality

(A) Schematic of the N1ICD transgenic allele. The transgene consists of N-terminal fusion of Myc epitope tag to aa1810-2556 of the mouse N1ICD lacking the RAM domain. (B) Immunoblot analysis showing Myc-N1ICD expression in *N1ICD;hGFAP-cre* embryo brains. (C) Realtime RT-PCR analysis of control and *N1ICD;hGFAP-cre* littermate cortices at E15.5. p-values = 0.0774 (*N1ICD*), 0.0495 (*Hes1*), 0.0218 (*Hes5*), 0.9741 (*Hey1*), 0.6529 (*Hey2*). (D) Realtime RT-PCR analysis of control and *N1ICD;hGFAP-cre* littermate cerebella at E15.5. p-values = 0.033 (*N1ICD*), 0.0397 (*Hes1*), 0.1663 (*Hes5*), 0.4509 (*Hey1*), 0.0004 (*Hey2*). (E) Survival curve for *N1ICD;hGFAP-cre* transgenic mice, compared to all other control littermates. (F) Gross image of control and *N1ICD;hGFAP-cre* mice brains at p20. Dotted lines mark the cortex and cerebellum. (G) Hematoxylin and eosin staining of coronal sections of forebrain at low magnification showing hypoplastic and disorganized neocortex and hippocampus, lacking dentate gyrus. Lower panels show a higher magnification of the cortex. Sagittal views of control and *N1ICD;hGFAP-cre* cerebellum showing hypoplasia and heterotopia in the transgenic brain. Boxed areas in the in the upper panels of the cerebella are shown in higher magnification below. Abbreviations: ctx: cortex, hp: hippocampus, thal: thalamus, CB: cerebellum. Scale bars=500 μm. Error bars show standard error mean. * denotes p<0.05.

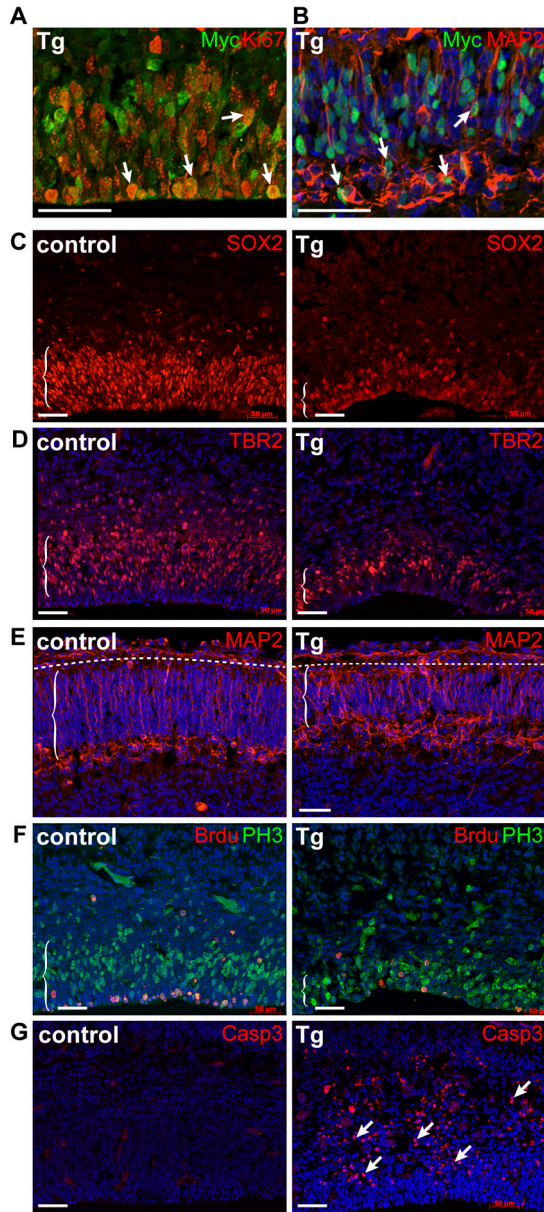


Figure 2. *NIICD* expression increases apoptosis and reduces the number of proliferating cells and neurons in the developing cortex

Immunofluorescence analyses with markers for: (A) the transgene, Myc, and proliferating cells (Ki67), (B) the transgene and differentiating neurons (MAP2), (C) neural stem cells (SOX2), (D) intermediate progenitors (TBR2), (E) neurons (MAP2), and (F) proliferation (PH3: M-phase, BrdU 1hour labeling: S-phase), (G) apoptosis (cleaved caspase 3). All images show coronal sections of cortices from E15.5 control and *NIICD;hGFAP-cre* littermates. Arrows point to positively stained cells. Dotted lines in (E) mark the pial surface interface. Scale bar = 50µm.

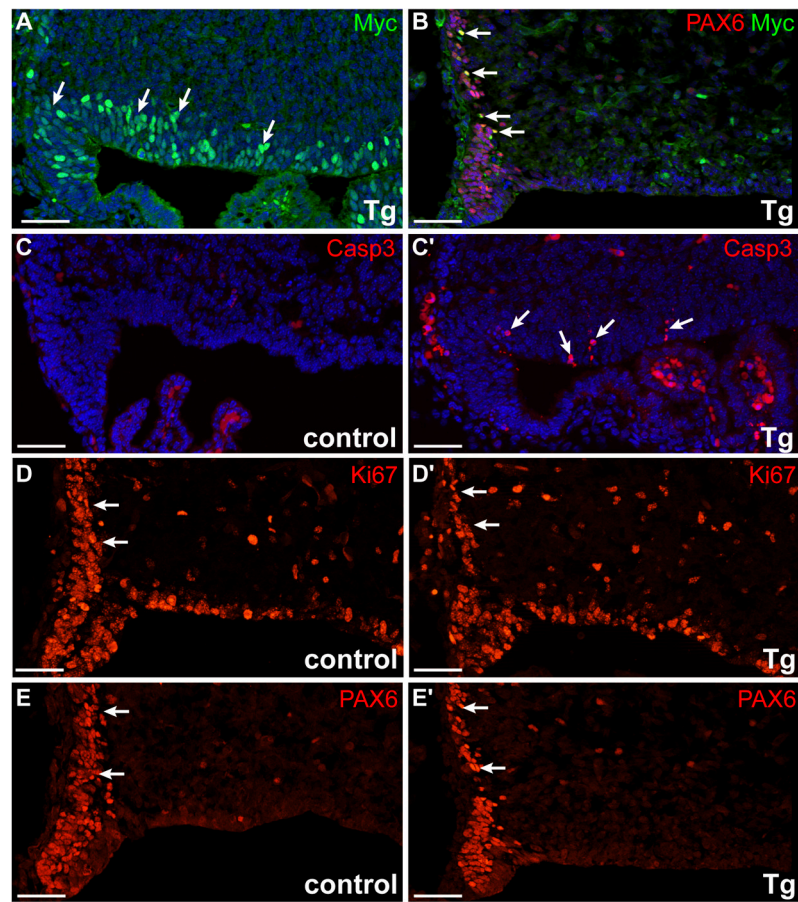


Figure 3. Ectopic expression of N1ICD induces apoptosis and reduces the number of neural precursors in the developing cerebellum

Immunofluorescence analyses of E14.5 cerebella with antibodies against: (A) the transgene (Myc) in the neuroepithelium, (B) Myc and PAX6 in early EGL precursors, (C) cleaved caspase 3, (D) proliferating cells (Ki67), and (E) neural precursor marker PAX6 at matching levels. All images show sagittal sections of rhombic lip region in control and *NIICD;hGFAP-cre* littermates. Arrows point to positively stained cells. Scale bar = 50 μ m.

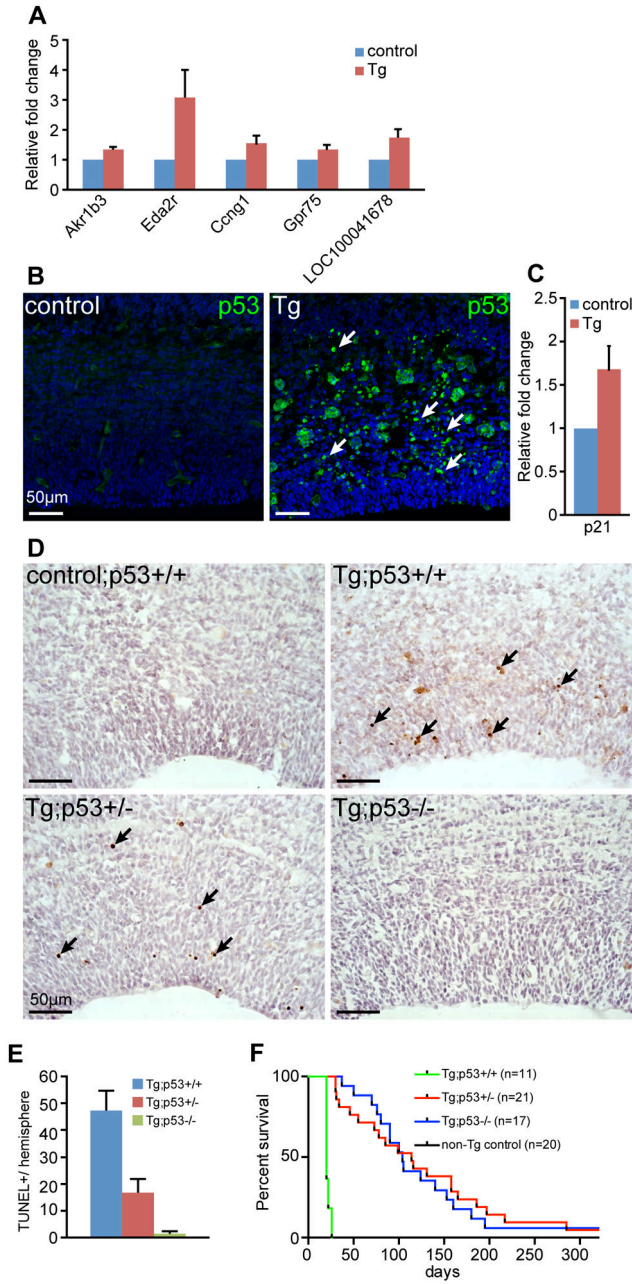


Figure 4. p53 is essential for NIICD-induced apoptosis

(A) Realtime RT-PCR analysis of genes up-regulated in *NIICD;hGFAP-cre* cortices at E13.5. (B) immunofluorescence analysis with an antibody against p53 protein, showing coronal sections through E15.5 control and *NIICD;hGFAP-cre* cortices. Arrows point to p53+ cells. (C) Realtime RT-PCR analysis of a p53 target gene, *Cdkn1a/p21*, in control and littermate *NIICD;hGFAP-cre* cortices. (D) TUNEL staining of control and transgenic (Tg: *NIICD;GFAP-cre*) cortices at E15.5 in p53 wildtype, heterozygous, and homozygous backgrounds. Arrows point to TUNEL+ cells. (E) Quantitation of TUNEL+ cells in each hemisphere. >8 hemisphere sections were counted for each genotype. (F) Kaplan-Meier survival curves of *NIICD;GFAP-cre;p53* wildtype, heterozygous, and homozygous mice. Scale bar = 50µm.

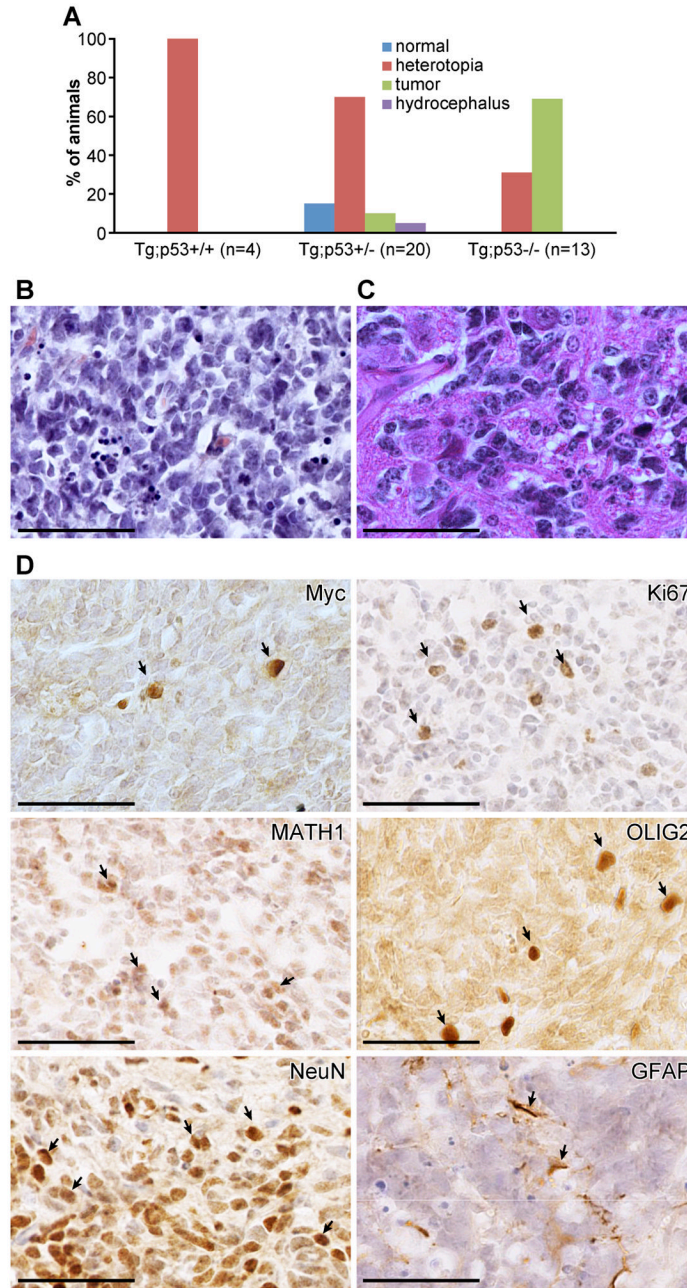


Figure 5. N1ICD transgenic mice with reduced *p53* dose develop spontaneous medulloblastomas (A) Distribution of mice with normal brain, hydrocephalus, heterotopia, and medulloblastomas among *N1ICD;hGFAP-Cre;p53* wildtype, heterozygous, and homozygous mice. (B, C) Hematoxylin and eosin staining of medulloblastomas that form in *N1ICD;GFAP-Cre;p53+/-* and *N1ICD;GFAP-Cre;p53-/-* mice. (D) Immunohistochemical analyses of N1ICD medulloblastomas with markers for the transgene (Myc), proliferation (Ki67), EGL-progenitors (ATOH1/MATH1), neural stem/progenitors (OLIG2), neurons (NeuN), and glia (GFAP). Scale bar = 50 μ m.

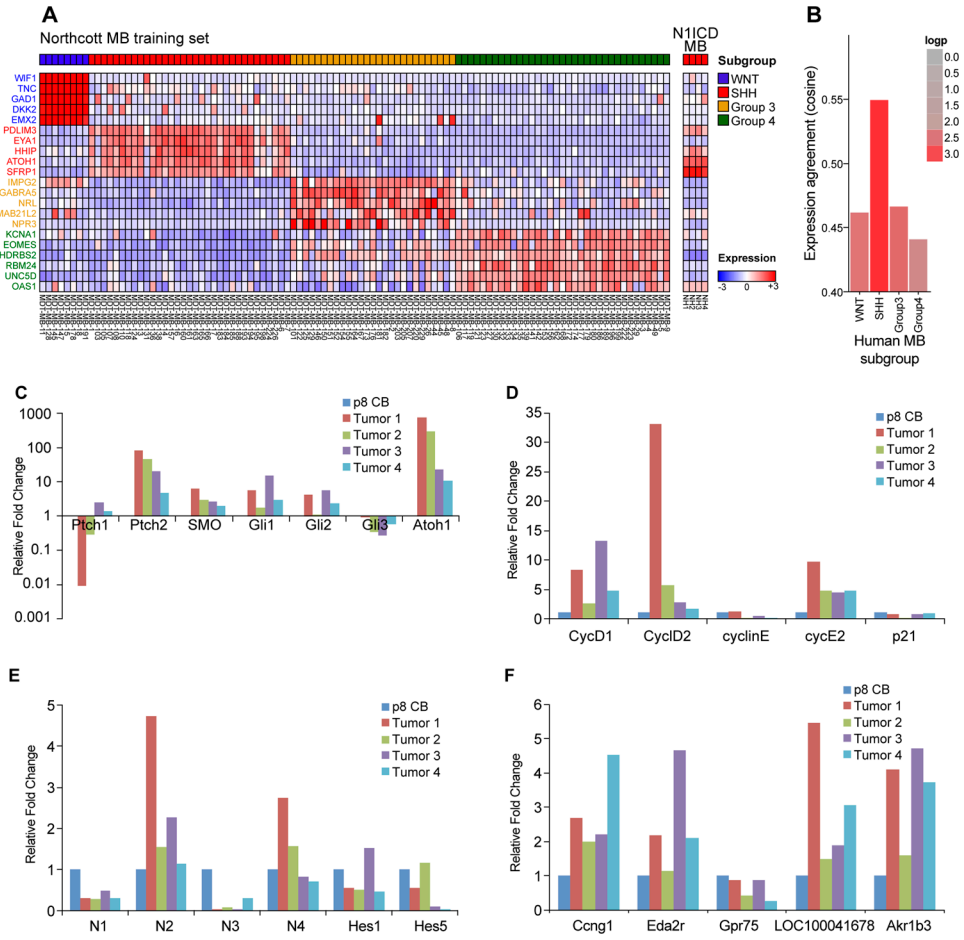


Figure 6. N1ICD-induced medulloblastomas most closely model the SHH-subgroup of human medulloblastomas

(A) Microarray analysis of N1ICD-induced medulloblastomas, compared against signature genes (Northcott MB training set) that distinguish the 4 molecular subgroups in human medulloblastomas. (B) Expression agreement analysis of N1ICD-induced tumors against the human medulloblastoma subgroups shows the highest correlation to the SHH-subtype. (C–E). Realtime RT-PCR analysis on RNAs isolated from four independent N1ICD-induced medulloblastomas. Expression levels are normalized against wildtype cerebellum at postnatal day 8. (C) SHH pathway genes, (D) cell cycle regulators, (E) Notch pathway genes, (F) genes downstream of N1ICD expression in *N1ICD;hGFAP-cre* cortices.